Self-assembly of Ni(II) porphine molecules on the Ag/Si(111)-$(\sqrt{3} \times \sqrt{3})R30^{\circ}$ surface studied by STM/STS and LEED

2008 J. Phys.: Condens. Matter 20 015003

(http://iopscience.iop.org/0953-8984/20/1/015003)

J. Phys.: Condens. Matter **20** (2008) 015003 (6pp) doi:10.1088/0953-8984/20/01/015003

Self-assembly of Ni(II) porphine molecules on the Ag/Si(111)-($\sqrt{3} \times \sqrt{3}$)R30° surface studied by STM/STS and LEED

J P Beggan[1], S A Krasnikov[1,2,5], N N Sergeeva[2], M O Senge[2] and A A Cafolla[1,3,4]

[1] School of Physical Sciences, Dublin City University, Glasnevin, Dublin 9, Republic of Ireland
[2] SFI Tetrapyrrole Laboratory, School of Chemistry, Trinity College Dublin, Dublin 2, Republic of Ireland
[3] Institute for Advanced Material Science (IAMS), Trinity College Dublin, Dublin 2, Republic of Ireland
[4] National Centre for Sensor Research (NCSR), Dublin City University, Glasnevin, Dublin 9, Republic of Ireland

E-mail: Sergey.Krasnikov@dcu.ie

Received 5 October 2007, in final form 9 November 2007
Published 29 November 2007
Online at stacks.iop.org/JPhysCM/20/015003

Abstract

The room-temperature growth and ordering of (porphyrinato)nickel(II) (nickel(II) porphine, NiP) molecules on the Ag/Si(111)-($\sqrt{3} \times \sqrt{3}$)R30° surface have been investigated using scanning tunnelling microscopy/spectroscopy (STM/STS) and low-energy electron diffraction (LEED). The results indicate a well-ordered molecular layer in which the porphyrin molecules have a flat orientation with the molecular plane lying parallel to the substrate and forming a hexagonal overlayer on the surface. STM and LEED data obtained from one monolayer (ML) of the NiP on the Ag/Si(111)-($\sqrt{3} \times \sqrt{3}$)R30° surface show the formation of two well-ordered mirror domains, each rotated either clockwise or counterclockwise by 7° with respect to the substrate. A hexagonal Moiré pattern was observed for the NiP overlayer due to long-range variation in the overlayer–substrate distance. It was found that the existence of such azimuthal rotation and the Moiré pattern are caused by a lattice mismatch between the substrate and the molecular overlayer, and a corresponding model is proposed. The NiP molecules forming the second monolayer maintain the same planarity and hexagonal ordering as the first molecular layer. Scanning tunnelling spectroscopy data obtained from the NiP overlayer on the Ag/Si(111)-($\sqrt{3} \times \sqrt{3}$)R30° surface show good agreement with density functional theory calculations.

1. Introduction

Porphyrins represent a class of flexible molecules with a nearly square planar core conformation and a two-dimensional conjugated π-electron delocalization [1–3]. Due to their interesting physicochemical properties, porphyrins are utilized in many technological applications such as molecular optoelectronic gates, molecular wires, photo-inducible energy or electron transfer systems, light-harvesting arrays for solar energy generation, one-dimensional conductors and semiconductors, enzyme models, oxidation catalysts, sensors, nonlinear optics and nanomaterials [2–7]. In particular, 3d transition metal (TM) porphyrins are widely used in the applications mentioned above, due to their unique electronic structure, which has been a subject of intense experimental and theoretical research during the last decade [8–12]. The central part of these complexes, including the 3d-atom and its nearest neighbours, is known to be their most reactive component, essentially responsible for the interesting properties exhibited by these compounds.

An important challenge in nanoscience is the ability to control the assembly of functional molecular species into

[5] Author to whom any correspondence should be addressed.

complex supramolecular structures. This controlled assembly of nanostructures offers a number of powerful approaches for the development of molecule-based devices [13]. An understanding of the porphyrin/inorganic interface with specific electrochemical or photochemical properties is a critical element that is required for optimizing their use in this area and in realizing new types of organic molecular devices, especially for photovoltaic applications. Of particular interest are the nature of the bonding between the porphyrin molecules and the surface, as reflected in the electronic charge distribution, and their geometric configuration at the interface. This information can be obtained by using a combination of scanning tunnelling microscopy and spectroscopy (STM and STS). STM is a highly local technique that has become a powerful tool for studying the adsorption geometry and the conformation and dynamics of single organic molecules and molecular assemblies on conducting substrates [14–23]. However, while these images elucidate the topographic structure of the interface, they provide little information about its electronic properties. STS, which involves measuring the tunnelling current at fixed tip–surface separation as the bias voltage is systematically varied ($I(V)$ spectroscopy), is one of the best tools for probing local electronic structure with molecular spatial resolution. STS is unique in that it allows both the filled and empty state density at the surface to be probed in a single measurement, providing local density of states information close to the Fermi level. This information is vital for understanding the properties of these 3d compounds and their utilization in molecular electronic devices.

In the present work, by using STM and LEED we focus for the first time on the molecular self-assembly of (porphyrinato)nickel(II) (NiP) on the Ag/Si(111)-($\sqrt{3} \times \sqrt{3}$)R30° surface in regimes from submonolayer to several monolayers in order to reveal the conformational behaviour of NiP molecules. STS is utilized to obtain information about the local density of states. The results of this work yield important information about the electronic and structural properties of the Ni(II) porphine molecules adsorbed on the Ag/Si(111)-($\sqrt{3} \times \sqrt{3}$)R30° surface.

2. Experimental details

The STM/STS experiments were performed at room temperature (RT), using a commercial instrument (Omicron Nanotechnology GmbH) in an ultra-high-vacuum (UHV) system consisting of an analysis chamber (with a base pressure of 2×10^{-11} mbar) and a preparation chamber (5×10^{-11} mbar). An electrochemically etched polycrystalline tungsten tip was used to record STM images in constant-current mode. The voltage V_{sample} corresponds to the sample bias with respect to the tip. No drift corrections have been applied to any of the STM images presented in this paper. The Si(111) substrate was p-type boron-doped with a resistivity in the range 0.1–1.0 Ω cm. Atomically clean Si(111)-(7 × 7) surfaces were prepared by *in situ* direct current heating to 1520 K after the samples were first degassed at 870 K for 12 h. The clean Si(111)-(7 × 7) surface was checked by low-energy electron diffraction (LEED) and STM before preparation of the Ag/Si(111)-($\sqrt{3} \times \sqrt{3}$)R30° surface. Silver (Goodfellow Metals, 5 N) was deposited by electron-beam evaporation from a molybdenum crucible onto the Si substrate, which was maintained at 770 K during the deposition. The cleanliness of the Ag/Si(111)-($\sqrt{3} \times \sqrt{3}$)R30° surface was verified by STM and LEED before deposition of the nickel(II) porphine.

Ni(II) porphine was synthesized according to a published procedure [24]. The NiP was evaporated in a preparation chamber isolated from the STM chamber at a rate of about 0.2 ML (monolayer) per minute from a tantalum crucible in a homemade deposition cell operated at a temperature of approximately 600 K. The total pressure during porphyrin deposition was in the 10^{-10} mbar range. Before evaporation, the NiP powder was degassed for about 10 h to remove water vapour.

Tunnelling spectra were acquired on a grid of specified points within an image. At each grid point the scan is interrupted during imaging; the feedback loop is switched off for $I(V)$ spectroscopy and, after a short delay time to allow stabilization of the current preamplifier, a voltage ramp is applied. In between the grid points the feedback is on and the STM operates in constant-current mode. While recording $I(V)$ spectra it was ensured that current measurements did not exceed the dynamic range of the current preamplifier. Before and after $I(V)$ or $z(V)$ spectra acquisition the quality of the surface was verified by STM imaging to ensure that no damage was done to the measured layer.

3. Results and discussion

Silver deposited on the Si(111)-(7 × 7) surface at elevated temperatures forms a ($\sqrt{3} \times \sqrt{3}$)R30° reconstruction [25, 26]. At room temperature the clean Ag/Si(111)-($\sqrt{3} \times \sqrt{3}$)R30° surface is well described by the honeycomb-chain-trimer model [25, 26]. The average length of the unit cell is 0.67 ± 0.05 nm [19, 20]. The clean Ag/Si(111)-($\sqrt{3} \times \sqrt{3}$)R30° surface was used as the substrate for the preparation of ultrathin (porphyrinato)nickel(II) layers. The Ag/Si(111)-($\sqrt{3} \times \sqrt{3}$)R30° was chosen since the porphyrin–substrate interaction is expected to be intermediate in strength between that on the clean Si surfaces and hydrogen passivated Si. On the former surfaces the molecules form covalent bonds and are unable to diffuse at room temperature [27], while on the latter the molecules diffuse freely and may form islands [28].

Figure 1 shows typical occupied state STM images of a single domain taken from approximately 1 ML of the NiP on the Ag/Si(111)-($\sqrt{3} \times \sqrt{3}$)R30° surface. The individual molecules appear as bright protrusions. NiP deposits on the surface forming large molecular domains (approximately 200 nm × 200 nm) with a well-defined hexagonal close-packed structure, as is seen clearly in figure 1. The formation of ordered domains of this extent indicates the presence of a strong intermolecular interaction, involving the hydrogen atoms of neighbouring NiP molecules, as well as a low diffusion barrier for the molecules on this surface at room temperature. In turn, a weaker bonding between NiP molecules and the substrate occurs through the molecular π-electron system. In the NiP overlayer each molecule has a flat

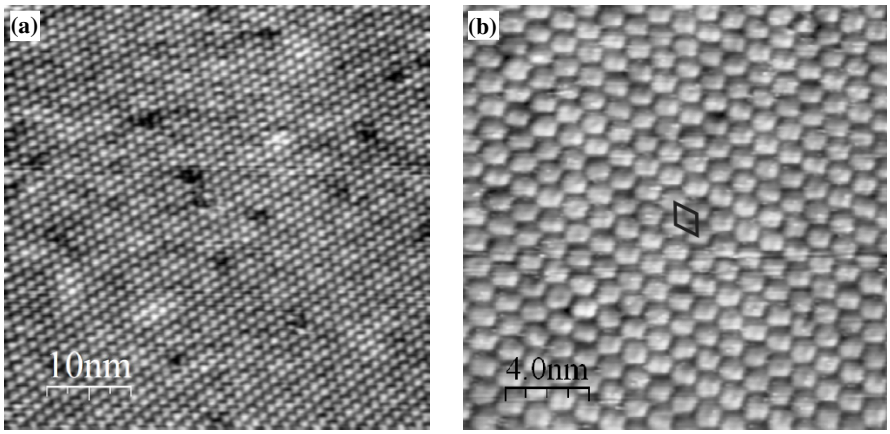

Figure 1. STM images taken from 1 ML of the NiP on the Ag/Si(111)-($\sqrt{3} \times \sqrt{3}$)R30° surface: (a) $I_t = 0.025$ nA, $V_{\text{sample}} = -1.0$ V, size 50 nm × 50 nm; (b) $I_t = 0.05$ nA, $V_{\text{sample}} = -2.0$ V, size 20 nm × 20 nm. The unit cell of the NiP overlayer is shown in black.

orientation on the surface with the molecular plane lying parallel to the substrate and surrounded by six neighbouring molecules. The unit cell of the NiP lattice (shown in black in figure 1(b)) contains one NiP molecule and has the following parameters: the unit cell vectors (**a** and **b**) are equal to 1.13 ± 0.05 nm, while the angle between them is 120° ± 1°, forming a hexagonal close-packed structure. The apparent size of an individual NiP molecule is approximately 1.1 nm.

Dual-scan-mode STM, where the surface topography can be obtained in both forward and backward scan directions, was exploited to obtain information about the ordering of the NiP overlayer relative to the substrate. By choosing appropriate sample bias conditions in this scanning mode, both the overlayer and the substrate can be imaged simultaneously. Examples of dual-scan-mode STM images obtained from the NiP overlayer on the Ag/Si(111)-($\sqrt{3} \times \sqrt{3}$)R30° surface are shown in figure 2. In this case, by using a small sample bias (−0.2 V) in the energy gap between the highest occupied (HOMO) and the lowest unoccupied molecular orbitals (LUMO) of the NiP molecule for the forward scan direction, it was possible to image the Ag/Si(111)-($\sqrt{3} \times \sqrt{3}$)R30° substrate through a molecular overlayer that appears transparent (figures 2(a) and (c)). The image formed at the same time in the backward scan direction, with a sample bias of −1.40 V, shows a typical NiP hexagonal overlayer structure (figures 2(b) and (d)). From these images it was found that the angle ϕ between the lattice vectors of the Ag/Si(111)-($\sqrt{3} \times \sqrt{3}$)R30° substrate and the NiP overlayer is equal to 7° ± 1°. This results from the lattice mismatch between the substrate and the molecular overlayer. The unit cell of the NiP overlayer (1.13 nm) was found to be 15% smaller than twice the unit cell of the substrate (0.67 nm). The intermolecular bonding appears to be stronger than the molecule–substrate bonding, which is usual for low-reactivity substrates such as the Ag-passivated Si. This low reactivity of the substrate allows the deposited NiP molecules to be quite mobile. It makes room-temperature STM imaging of the molecules difficult at low surface coverage, because individual molecules can easily be dragged by the STM tip. Such mobility on the surface and the presence of strong intermolecular interaction make the formation of a close-packed layer favourable. In turn, this close-packed layer is weakly bonded to the Ag/Si(111)-($\sqrt{3} \times \sqrt{3}$)R30° surface. Thus, the lateral intermolecular interactions dominate over site-specific adsorption on the substrate, leading to azimuthal rotation of the NiP molecular domains mediated by the interaction with the Ag/Si(111)-($\sqrt{3} \times \sqrt{3}$)R30° surface in order to minimize the inequivalent number of adsorption sites.

Two well-ordered domains of NiP, having threefold symmetry, were observed. Each NiP domain was rotated either clockwise or counterclockwise by 7° with respect to the substrate, as shown in figure 2. These two domains are mirror images of each other, with the mirror plane perpendicular to the surface and aligned along the close-packed direction of the latter. Furthermore, the LEED pattern obtained from 1 ML of the NiP on the Ag/Si(111)-($\sqrt{3} \times \sqrt{3}$)R30° surface shows two sets of diffraction spots, each forming a hexagonal pattern (see figure 3(a)). These hexagonal patterns represent two mirror NiP domains, confirming the dual-scan-mode STM observations. The angle Φ between two hexagons observed in the LEED pattern is equal to 14°, which is in excellent agreement with data obtained from STM dual-scan-mode images. Measurements of the lattice constants of the NiP overlayer, determined from a comparative analysis of LEED images from the overlayer and the substrate, are in agreement with the values obtained by STM. The clarity of the LEED pattern indicates the presence of a highly ordered NiP surface. A corresponding model for the NiP molecular overlayer (in the case of the clockwise rotated domain) was proposed and is shown in figure 3(b).

Figure 4(a) shows a long-range intensity modulation, a hexagonal Moiré pattern with periodicity of approximately 4.5 nm, observed in large-area scans of the NiP overlayer. A similar Moiré pattern is also visible in figure 1(a). In both images, two hexagonal structures coexist: one with a short periodicity and a second with a longer periodicity. The short-periodicity hexagonal structure is due to the NiP molecules, while the long-periodicity Moiré structure is observed as a periodic modulation in the apparent height of the molecules produced by the superposition of the hexagonal NiP lattice

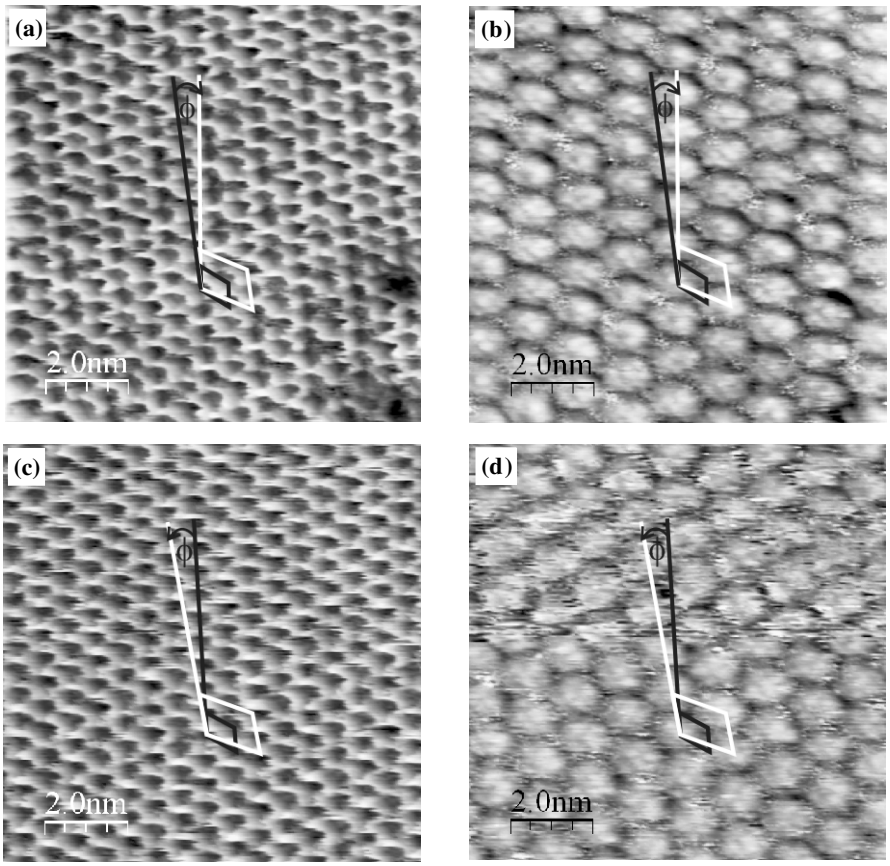

Figure 2. STM dual-scan-mode images obtained from 1 ML of the NiP on the Ag/Si(111)-($\sqrt{3} \times \sqrt{3}$)R30° surface. Images (a) and (c) are obtained in the forward scan direction: $I_t = 0.25$ nA, $V_{\text{sample}} = -0.20$ V, size 10 nm × 10 nm. Images (b) and (d) are obtained in the backward scan direction: $I_t = 0.25$ nA, $V_{\text{sample}} = -1.40$ V, size 10 nm × 10 nm. Images (a) and (b) represent the NiP domain rotated clockwise with respect to the substrate. Images (c) and (d) represent the NiP domain rotated counterclockwise. The unit cells and close-packed directions are shown in black (substrate) and white (NiP overlayer).

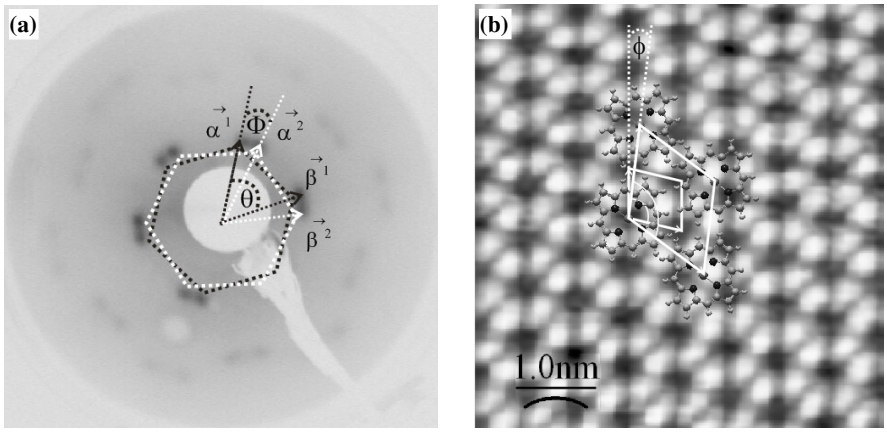

Figure 3. LEED pattern from 1 ML of the NiP on the Ag/Si(111)-($\sqrt{3} \times \sqrt{3}$)R30° surface acquired at a kinetic energy of 14.8 eV (a). The black and white hexagons represent the two NiP domains rotated clockwise and counterclockwise relative to the substrate. The angle Φ between the two domains is equal to 14°. Schematic representation of the NiP overlayer (clockwise rotated domain) superimposed on an STM image of the Ag/Si(111)-($\sqrt{3} \times \sqrt{3}$)R30° surface (b). The substrate and the molecular overlayer unit cells are shown in white. The angle ϕ between them is equal to 7°.

on the underlying hexagonal lattice of the Ag/Si(111)-($\sqrt{3} \times \sqrt{3}$)R30° substrate. The presence of a low diffusion barrier and Moiré patterning indicates weak site-specific coupling of the molecular overlayer with the underlying substrate.

Previous STM observations of substituted porphyrin molecules performed to date on different substrates show a complex behaviour and ordering of the molecules, which depends on the substrate reactivity and the nature of the

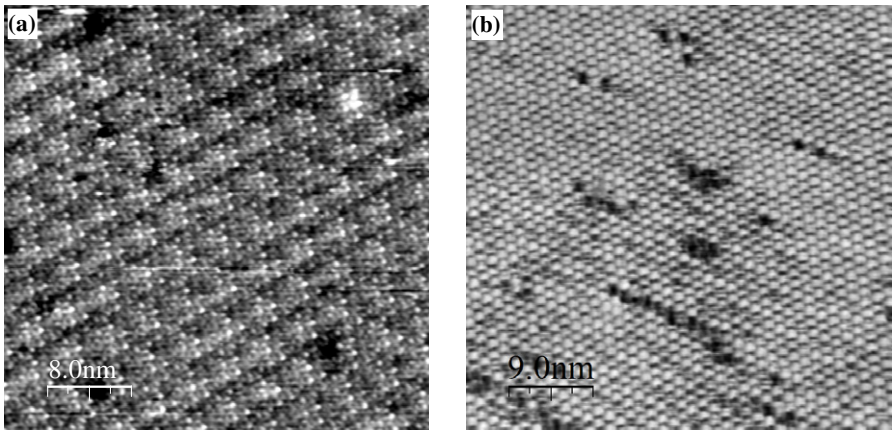

Figure 4. STM image taken from 1 ML of the NiP on the Ag/Si(111)-($\sqrt{3} \times \sqrt{3}$)R30° surface showing the Moiré pattern (a): $I_t = 0.5$ nA, $V_{\text{sample}} = -1.4$ V, size 40 nm × 40 nm. STM image taken from 2 ML of the NiP on the Ag/Si(111)-($\sqrt{3} \times \sqrt{3}$)R30° surface (b): $I_t = 0.75$ nA, $V_{\text{sample}} = -1.75$ V, size 45 nm × 45 nm.

outer substituents attached to the porphyrin macrocycle [15–18, 21–23, 29, 30]. On passive substrates such as highly oriented pyrolytic graphite (HOPG), silver and gold porphyrin molecules form oblique [15–17, 21–23, 29], hexagonal [17, 18] and square [23, 30] close-packed structures or elongated molecular-like wires [22]. In the case of 5,10,15,20-tetrapyridylporphyrins adsorbed on the Ag(111) surface [29] and 5,10,15,20-tetra(3,5-bis-tert-butylphenyl)porphyrins adsorbed on the Cu(100) surface [30] two mirror molecular domains were observed azimuthally rotated with respect to the substrate, similar to the NiP case. For both substituted porphyrin molecules the formation and azimuthal rotation of such close-packed domains was mediated by rotation and tilt of substituents attached to the porphyrin macrocycle and by molecular–substrate interaction, respectively. Furthermore, the tetrapyridylporphyrin layer on the Ag(111) surface shows quasihexagonal Moiré pattern [29].

Figure 4(b) shows a typical occupied state STM image taken from approximately 2 ML of the NiP on the Ag/Si(111)-($\sqrt{3} \times \sqrt{3}$)R30° surface. It is clearly seen that the second NiP layer preserves the same planarity and hexagonal ordering as the first molecular layer.

Figure 5 shows a comparison between the normalized conductivity spectrum $(\mathrm{d}I/\mathrm{d}V)/(I/V)$ and the $z(V)$ spectra recorded from the NiP overlayer on the Ag/Si(111)-($\sqrt{3} \times \sqrt{3}$)R30° surface. It is important to note that $I(V)$ and $z(V)$ spectroscopy are two different STM-based techniques which provide similar information about the density of states of the material, which is probed as a function of voltage (sample bias) through changes in the tunnelling current ($I(V)$) or the tip height ($z(V)$) [14, 31, 32]. The normalized conductivity spectrum was obtained by numerical differentiation of the $I(V)$ spectrum and is proportional to the density of states. Each spectrum is the result of averaging over a few hundred spectra taken within an image using a grid of specified points. Spectra 1 and 2 were recorded over the area of the image shown in figure 2(b). The normalized conductivity spectrum shows two prominent features observed at −1.2 and 0.9 V, representing the highest occupied and lowest unoccupied

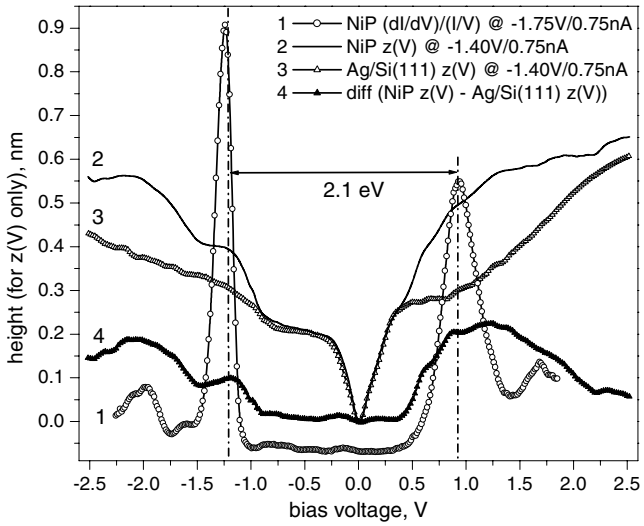

Figure 5. Normalized conductivity $(\mathrm{d}I/\mathrm{d}V)/(I/V)$ and $z(V)$ spectra recorded from 1 ML of the NiP on the Ag/Si(111)-($\sqrt{3} \times \sqrt{3}$)R30° surface (spectra 1 and 2, respectively). The $z(V)$ spectrum from the clean Ag/Si(111)-($\sqrt{3} \times \sqrt{3}$)R30° surface is shown in open triangles (spectrum 3). Spectrum 4 represents the difference between $z(V)$ spectra taken from the molecular overlayer and the substrate.

electronic states, respectively. Furthermore, this spectrum shows good agreement with the spectrum representing the difference between $z(V)$ spectra taken from the NiP overlayer and the Ag/Si(111)-($\sqrt{3} \times \sqrt{3}$)R30° surface.

The following peak assignment can be made by comparing these results with electronic structure calculations using density functional theory [9, 10]. The peak observed at −1.2 eV corresponds to the HOMO having a_{1g} symmetry. The unoccupied state situated at 0.9 eV is the LUMO having b_{1g} symmetry. The peak assignment was made keeping in mind that the Ni(II) porphine molecule has D_{4h} symmetry, which is preserved on the Ag/Si(111)-($\sqrt{3} \times \sqrt{3}$)R30° surface, as shown by STM images, since molecule–substrate interaction is weak, as discussed above. The chemical bonding of the nickel atom

with four pyrrole rings (having D_{4h} symmetry in NiP) results in the formation of four σ bonds due to in-plane mixing of ligand $2p\sigma$ states with Ni $3d_{z^2}+4s$, $3d_{x^2-y^2}$ and $4p_{x,y}$ states, which are described by the a_{1g}, b_{1g} and e_u MOs, respectively [8–10]. In this case the a_{1g} and b_{1g} MOs represent the HOMO and LUMO, respectively. An additional π bonding of the metal atom with the ligands is fulfilled by a covalent interaction of the Ni $3d_{xz,yz}$ orbitals with the out-of-plane ligand 2p orbitals, which is accompanied by a charge transfer from the metal atom into the ligands (π-back donation) [8, 33–35]. This covalent bonding results in a π-MO of e_g symmetry. The HOMO–LUMO band gap of the NiP obtained from STS data is equal to 2.1 eV, which is in excellent agreement with theoretical calculations [9, 10] and optical band gap measurements [24, 36].

In conclusion, the room temperature growth and ordering of (porphyrinato)nickel(II) on the Ag/Si(111)-($\sqrt{3}\times\sqrt{3}$)R30° surface have been investigated using STM, STS and LEED. A well-ordered molecular layer was obtained in which the NiP molecules have a flat orientation, with the molecular planes lying parallel to the surface, and form a hexagonal structure. STM and LEED data obtained from 1 ML of the NiP on the Ag/Si(111)-($\sqrt{3}\times\sqrt{3}$)R30° surface show the formation of two hexagonally ordered mirror domains, each rotated either clockwise or counterclockwise by 7° with respect to the substrate, which is caused by a lattice mismatch between the substrate and the molecular overlayer. The lateral intermolecular interactions dominate over site-specific adsorption on the substrate, leading to this azimuthal rotation in order to minimize the inequivalent number of adsorption sites and the local variation in the overlayer–substrate distance. STS data obtained from one monolayer of the NiP on the Ag/Si(111)-($\sqrt{3}\times\sqrt{3}$)R30° surface show good agreement with density functional theory calculations.

Acknowledgments

This work was supported by the Irish Higher Education Authority through the Programme for Research in Third Level Institutions (PRTLI) and by Science Foundation Ireland through the Research Frontiers Programme (grant number 06/RFP/PHY082 to AAC) and the Science Foundation Ireland Research Professorship (grant number 04/RPI/B482 to MOS). STM topographic images were processed using WSxM freeware [37].

References

[1] Hoard J L 1973 *Ann. New York Acad. Sci.* **206** 18
[2] Kadish K M, Smith K M and Guilard R (ed) 2000 *The Porphyrin Handbook* vol 1–10 (San Diego, CA: Academic)
[3] Senge M O 2006 *Chem. Commun.* 243
[4] Anderson H L 1999 *Chem. Commun.* 2323
[5] Lin V S Y, DiMagno S G and Therien M J 1994 *Science* **264** 1105
[6] Chen J, Reed M A, Rawlett A M and Tour J M 1999 *Science* **286** 1550
[7] Tsuda A and Osuka A 2001 *Science* **293** 79
[8] Krasnikov S A, Preobrajenski A B, Sergeeva N N, Brzhezinskaya M M, Nesterov M A, Cafolla A A, Senge M O and Vinogradov A S 2007 *Chem. Phys.* **332** 318
[9] Liao M-S and Scheiner S 2002 *J. Chem. Phys.* **117** 205
[10] Rosa A, Ricciardi G, Baerends E J and van Gisbergen S J A 2001 *J. Phys. Chem.* A **105** 3311
[11] de Jong M P, Friedlein R, Sorensen S L, Öhrwall G, Osikowicz W, Tengsted C, Jönsson S K M, Fahlman M and Salaneck W R 2005 *Phys. Rev.* B **72** 035448
[12] Polzonetti G, Carravetta V, Iucci G, Ferri A, Paolucci G, Goldoni A, Parent P, Laffon C and Russo M V 2004 *Chem. Phys.* **296** 87
[13] Barth J V 2007 *Annu. Rev. Phys. Chem.* **58** 375
[14] Krasnikov S A, Hanson C J, Brougham D F and Cafolla A A 2007 *J. Phys.: Condens. Matter* **19** 446005
[15] Auwärter W, Weber-Bargioni A, Brink S, Riemann A, Schiffrin A, Ruben M and Barth J V 2007 *Chem. Phys. Chem.* **8** 250
[16] Spillmann H, Kiebele A, Stöhr M, Jung T A, Bonifazi D, Cheng F and Diederich F 2006 *Adv. Mater.* **18** 275
[17] Elemans J A W, van Hameren R, Nolte R J M and Rowan A E 2006 *Adv. Mater.* **18** 1251
[18] Ogunrinde A, Hipps K W and Scudiero L 2006 *Langmuir* **22** 5697
[19] Sheerin G and Cafolla A A 2005 *Surf. Sci.* **577** 211
[20] Guaino Ph, Cafolla A A, Carty D, Sheerin G and Hughes G 2003 *Surf. Sci.* **540** 107
[21] Scudiero L, Barlow D E and Hipps K W 2002 *J. Phys. Chem.* B **106** 996
[22] Yokoyama T, Yokoyama S, Kamikado T, Okuno Y and Mashiko S 2001 *Nature* **413** 619
[23] Jung T A, Schlittler R R and Gimzewski J K 1997 *Nature* **386** 696
[24] Unger E, Bobinger U, Dreybrodt W and Schweitzer-Stenner R 1993 *J. Phys. Chem.* **97** 9956
[25] Wilson R J and Chiang S 1987 *Phys. Rev. Lett.* **58** 369
[26] van Loenen E J, Demuth J E, Tromp R M and Hamers R J 1987 *Phys. Rev. Lett.* **58** 373
[27] Kanai M, Kawai T, Motai K, Wang X D, Hashizume T and Sakura T 1995 *Surf. Sci.* **329** L619
[28] Suzuki Y, Hietschold M and Zahn D R T 2006 *Appl. Surf. Sci.* **252** 5449
[29] Auwärter W, Weber-Bargioni A, Riemann A, Schiffrin A, Gröning O, Fasel R and Barth J V 2006 *J. Chem. Phys.* **124** 194708
[30] Sekiguchi T, Wakayama Y, Yokoyama S, Kamikado T and Mashiko S 2004 *Thin Solid Films* **464/465** 393
[31] Feenstra R 1994 *Phys. Rev.* B **50** 4561
[32] Alvarado S F, Seidler P F, Lidzey D G and Bradley D D C 1998 *Phys. Rev. Lett.* **81** 1082
[33] Cotton F A and Wilkinson G 1972 *Advanced Inorganic Chemistry* (New York: Wiley)
[34] Vinogradov A S, Preobrajenski A B, Knop-Gericke A, Molodtsov S L, Krasnikov S A, Nekipelov S V, Szargan R, Hävecker M and Schlögl R 2001 *J. Electron Spectrosc. Relat. Phenom.* **114–116** 813
[35] Vinogradov A S, Preobrajenski A B, Krasnikov S A, Chassé T, Szargan R, Knop-Gericke A, Schlögl R and Bressler P 2002 *Surf. Rev. Lett.* **9** 359
[36] Edwards L, Dolphin D H and Gouterman M 1970 *J. Mol. Spectrosc.* **35** 90
[37] Horcas I, Fernandez R, Gomez-Rodriguez J M, Colchero J, Gomez-Herrero J and Baro A M 2007 *Rev. Sci. Instrum.* **78** 013705